IEEE Transactions on Quantum Engineering

Received 25 July 2023; revised 18 January 2024; accepted 27 February 2024; date of publication 7 March 2024; date of current version 23 April 2024.

Digital Object Identifier 10.1109/TQE.2024.3374251

Quantum Fuzzy Inference Engine for Particle Accelerator Control

GIOVANNI ACAMPORA[1,2] (Senior Member, IEEE), MICHELE GROSSI[3], MICHAEL SCHENK[4], AND ROBERTO SCHIATTARELLA[1,2] (Student Member, IEEE)

[1]Department of Physics "Ettore Pancini," University of Naples Federico II, 80126 Naples, Italy
[2]Istituto Nazionale di Fisica Nucleare, 80126 Naples, Italy
[3]IT Department, European Organization for Nuclear Research, 1211 Meyrin, Switzerland
[4]Beams Department, European Organization for Nuclear Research, 1211 Meyrin, Switzerland

Corresponding author: Roberto Schiattarella (e-mail: roberto.schiattarella@unina.it).

The work of Roberto Schiattarella was supported by the IEEE Computational Intelligence Society Graduate Student Research Grants. The work of Michele Grossi was supported by the European Organization for Nuclear Research through the Quantum Technology Initiative.

ABSTRACT Recently, quantum computing has been proven as an ideal theory for the design of fuzzy inference engines, thanks to its capability to efficiently solve the rule explosion problem. In this scenario, a quantum fuzzy inference engine (QFIE) was proposed as a quantum algorithm able to generate an exponential computational advantage over conventional fuzzy inference engines. However, there are no practical demonstrations that the QFIE can be used to efficiently manage complex systems. This article bridges this gap by using, for the very first time, the QFIE to control critical systems such as those related to particle accelerator facilities at the European Organization for Nuclear Research (CERN). As demonstrated by a series of experiments performed at the T4 target station of the CERN Super Proton Synchrotron fixed-target physics beamline and at the Advanced Proton Driven Plasma Wakefield Acceleration Experiment, the QFIE is able to efficiently control such an environment, paving the way for the use of fuzzy-enabled quantum computers in real-world applications.

INDEX TERMS Quantum computing, fuzzy control systems, particle accelerators.

I. INTRODUCTION

Fuzzy set and logic theory introduced by Zadeh [1], [2] has the capability of model classes of objects that do not have precisely defined criteria of membership, in a way to mimic human thinking on computers. Starting from Zadeh's theory of fuzzy logic, fuzzy-rule-based systems (FRBSs) have been developed, and they have found a widespread set of applications in the field of automatic control and decision making [3], [4]. The reason for this success can be explained by the fact that expert knowledge is easily introduced into these systems using *fuzzy rules*. Despite their success, FRBSs suffer from the so-called *fuzzy rule explosion problem:* the number of rules in an FRBS grows exponentially with the number of variables that make up the system. This problem severely limits the ability of an FRBS to handle systems with a large number of variables. Recently, the quantum computing paradigm has been explored to implement a new generation of efficient fuzzy inference engines (FIEs) to overcome the critical limitation of FRBSs potentially. The first quantum fuzzy inference engine (QFIE) has been developed in [5]: it uses the massive parallelism provided by quantum phenomena, such as superposition and entanglement, to reach an exponential advantage in computing fuzzy rules with respect to the classical counterpart. However, this quantum-based fuzzy engine has only been tested on control applications characterized by simple dynamics, such as inverse pendulum, and, as a result, there is no concrete evidence of its operational usability. This article fills this gap by exploring the potential of QFIE in an important area such as the automatic control of particle accelerators at the European Organization for Nuclear Research (CERN), achieving a twofold result. On the one hand, this research proves that the QFIE can be used reliably in complex application scenarios; on the other hand, it demonstrates that FRBSs are suitable methods for supporting particle accelerator operation at CERN. The suitability of QFIE for the automatic control of particle accelerators has been demonstrated in two different experimental settings, related to two different CERN facilities: the

© 2024 The Authors. This work is licensed under a Creative Commons Attribution-NonCommercial-NoDerivatives 4.0 License.
For more information, see https://creativecommons.org/licenses/by-nc-nd/4.0/

T4 target station at the North Area TT24 fixed-target physics beamline served by the Super Proton Synchrotron (SPS) [6] and the electron beamline of the Advanced Proton Driven Plasma Wakefield Acceleration Experiment (AWAKE) [7]. In the first case study, two configurations of QFIE were tested. The former exploited a quantum simulator and the latter was computed on a real quantum computer, namely, *IBMQ Montreal*. In the AWAKE case study, the QFIE was used to implement a more complex 10-D control system, and due to the limitations that characterize the current generation of quantum computers, known as noisy intermediate-scale quantum (NISQ) devices [8], the tests were performed just by using a quantum simulation. In these first experiments, both the T4 target station and the AWAKE environments were simulated and the suitability of QFIE in dealing with those has been assessed in terms of sample efficiency, i.e., the number of actions performed by the controller to achieve the desired behavior of the particle beam. Indeed, optimizing this kind of efficiency is essential in the context of accelerator operation to minimize the impact on the beam time available for physics experiments. Remarkably, the level of sample efficiency achieved by the QFIE in the above simulations was such that it allowed successful real-time control of the actual AWAKE facility, as demonstrated by the experimentation described in Section V.

The rest of this article is organized as follows. Section II presents an analysis of the literature on the integration of fuzzy logic and quantum computing. Section III summarizes the basic concepts related to the quantum computing and the main aspects of the QFIE. Section IV shows how QFIE-based FRBSs can be used to control particle accelerators and reports on the experiments performed for the simulated T4 target station and AWAKE environments. Section V shows the experiments on the real AWAKE facility. Finally, Section VI concludes this article.

II. RELATED WORKS

Quantum computing is becoming more and more a computational paradigm useful to develop a new generation of powerful and efficient computational intelligence algorithms: for instance, huge efforts have been done in the context of quantum neural networks [9], [10], [11], as well as in quantum evolutionary computing [12], [13]. In both areas, these works show a potential advantage in using this new quantum computational intelligence framework over the classical counterpart. On the other hand, quantum fuzzy logic is a relatively new and underexplored field. In recent years, several approaches have been proposed that aim to leverage the relationship between quantum mechanics and fuzzy set theory for mutual benefit [14], [15], [16], [17]. Broadly speaking, three research paths have emerged: the first involves using fuzzy set theory to simulate and model physical quantum systems [18], [19]; the second uses fuzzy-logic-based techniques to improve the current status of quantum computers, by means of algorithms useful to distribute quantum circuits [20] or to mitigate quantum error [21] among the others; and the last path involves exploring quantum computing approaches to enhance the performance of traditional fuzzy systems. Our interests focus on this latter area, which is hereafter deeply analyzed.

One of the first applications of quantum computing to improve the computational performance of fuzzy systems is presented by Rigatos and Tzafestas [22]. This study involves substituting quantum operations for certain operations used in particular FIEs. Despite the encouraging theoretical outcomes presented in [22], there were no appropriate quantum devices or simulators accessible at the time of research to enable experimental verification in the field.

Subsequent works have concentrated on implementing quantum fuzzy logic operators using various quantum computational paradigms. Some researchers employed a quantum circuit model for the implementation of these operators, as seen in [23] and [24], while others leveraged different quantum computational models, such as quantum annealing, as seen in [25] and [26]. Although these studies demonstrated that quantum operations could perform fundamental logic operations between fuzzy sets, none of them developed an efficient quantum algorithm for executing FIEs on quantum computers. One of the earliest studies in this direction, as mentioned in [27], employed Grover's algorithm to implement a fuzzy system that relied on a lookup table. Despite being the first attempt to use a well-known quantum algorithm to implement a whole fuzzy system, this approach was limited in scope. The input–output relationships that exist in the lookup had to be generated using classical computation, which hindered the potential computational advantage from the quantum implementation of FRBSs. Finally, such a computational advantage has been proven very recently in [5]. A deep description of the algorithm proposed in this article is carried out in Section III-B. However, the main goal of the aforementioned work was the theoretical proposal of an innovative QFIE, which has been tested in very easy case studies and just by noiseless simulations of the quantum circuits implementing the algorithm. According to this analysis of the state of the art, this work represents the very first attempt to use the QFIE in [5] for the control of real and complex environments, such as those related to particle accelerators at the CERN facilities. Moreover, the proposed work shows also the first real execution of the QFIEs on real quantum devices from the IBM Q family [28].

III. BASIC CONCEPTS

This section aims to introduce the basic concepts of quantum computing useful to understand the QFIE algorithm, highlighting also the hardware limitations of the current quantum devices. Successively, a brief description of the QFIE proposed in [5] is carried out.

A. QUANTUM COMPUTING

Quantum computing manipulates and stores information by using qubits, the basic information unit of this innovative computational paradigm. The main peculiarity of qubits is

IEEE Transactions on Quantum Engineering

that, unlike the classical bits, they can live in a superposition of states. Formally, a qubit is described by a vector of a Hilbert space $\mathcal{H}$: according to the bra-ket notation, such a vector is expressed as follows:

$$|\psi\rangle = \alpha|0\rangle + \beta|1\rangle \tag{1}$$

where the set $\{|0\rangle, |1\rangle\}$ forms a basis of $\mathcal{H}$, while α and β are complex coefficients. When a quantum state is measured, it collapses into one of its basis states with a probability equal to the squared modulus of the related coefficient. The result of the measurement operation is, therefore, a classical bit 0 or 1 obtained with a probability $|\alpha|^2$ or $|\beta|^2$, respectively. One of the most powerful peculiarities of quantum computers is the fact that when more qubits are used simultaneously, the size of the Hilbert space in which the quantum state lives increases exponentially with the number of qubits. This means that by considering n qubits, the quantum state describing the system is expressed as follows:

$$|\psi\rangle = \sum_{i=0}^{2^n-1} \alpha_i |i\rangle \tag{2}$$

where i denotes the integer representation of the n-dimensional bit string, and the coefficients α_i have the same meaning as the 1-D case described above.

Quantum states can be manipulated by quantum gates as well as classical bits can be manipulated by means of logical gates [29]. By definition, quantum gates are represented by unitary matrices that act on a state as follows:

$$U|\psi\rangle = U \sum_{i=0}^{2^n-1} \alpha_i |i\rangle. \tag{3}$$

A more in-depth description of these gates is out of the scope of this article but can be found in [29]. Overall, a quantum algorithm is a collection of quantum gates acting on several qubits. Like other important quantum algorithms [30], [31], the QFIE is based on the concept of quantum oracle. A quantum oracle U_h represents a black box (composed of one or more quantum gates) implementing a certain Boolean function $h(x) : \{0, 1\}^n \rightarrow \{0, 1\}^m$. Formally, considering two quantum registers composed of n and m qubits, respectively, the action of U_h can be expressed as

$$U_h \sum_x |x, \bar{0}\rangle = \sum_x |x, h(x)\rangle \tag{4}$$

where $|\bar{0}\rangle$ represents a quantum register whose qubits are in the quantum state $|0\rangle$. In other words, by means of quantum oracles, it is possible to evaluate the Boolean function $h(x)$ on all the possible n-dimensional inputs simultaneously, with just one query to the oracle thanks to the superposition of the input state.

In the end, the resulting quantum circuit is measured, and usually, this procedure is repeated several times to estimate the probability distribution encoded in the output quantum state.

In the past few years, various quantum hardware have been made available through cloud services by several major industries. However, these primordial quantum devices are denoted as NISQ computers [8]. The label refers to the limited amount of qubits of these devices and also to the high level of noise that occurs during the computation of quantum circuits. Recently, a lot of improvements have been made in the development of quantum hardware: for instance, IBM has recently announced the first superconductive chip composed of more than 1000 qubits. However, this number of qubits is still too low for implementing error correction codes, according to actual protocols, directly on hardware. On the other hand, attempts to simplify quantum circuits to be executed on actual NISQ devices have been presented. One example is the D-NISQ reference model introduced in [32]. This architecture offers a reference model for distributing quantum computation in smaller quantum circuits that can then be executed on different quantum processors. The integration of the different outputs is in the end classically performed by means of the *information fusion* layer, which returns the output of the original problem to solve. As shown in Section IV-B, such a model is used in this work for enabling the development of a quantum fuzzy control system able to control a 10-D environment such as the one of the AWAKE experiment at CERN.

B. QUANTUM FUZZY INFERENCE ENGINE

An FRBS is a type of control system that incorporates fuzzy logic principles to handle complex and uncertain environments. It is a powerful methodology used in various fields, including engineering [33], robotics [34], and finance [35]. Traditional control systems rely on crisp logic and precise mathematical models to make decisions and control processes. However, in many real-world scenarios, the inputs and outputs of a system are not easily quantifiable or precise. FRBSs provide a flexible and intuitive approach to dealing with such situations. In detail, an FRBS performs a mapping between input and output variables by using fuzzy if–then rules [36]. In a classical multi-input single-output fuzzy system composed of n input variables $X_1, X_2, \ldots, X_n$ and one output variable Y, the general rule can be written as follows:

$$\begin{aligned} &\text{IF } (X_1 \text{ is } T_{i1}) \text{ and } (X_2 \text{ is } T_{i2}) \text{ and} \\ &\quad \ldots \text{ and } (X_n \text{ is } T_{rn}) \text{ THEN } Y \text{ is } T_{i_Y} \end{aligned} \tag{5}$$

where T_{ij} is the ith linguistic term defined in the universe of discourse of X_j for $j = 1, \ldots n$, and T_{i_Y} is the ith linguistic term defined in the universe of discourse of Y. Considering that each linguistic term is described by a fuzzy set, the workflow of a classical FRBS can be summarized in three main steps.

1) *Fuzzification:* Given a set of n crisp inputs $x_1, x_2, \ldots x_n$, these values are fuzzified by determining the degree of membership in each fuzzy set using the related membership functions.
2) *Inference:* The FIE performs the following operations:

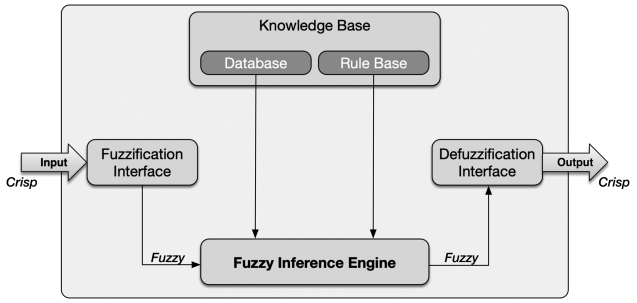

FIGURE 1. Architecture of an FRBS [5].

a) evaluation of the *antecedent* part of all the fuzzy rules, where "*antecedent*" denotes the fuzzy proposition before[1] the "THEN" keyword in (5);
b) computation of fuzzy output for each rule by applying the implication operator;
c) aggregation of all the rule outputs in the output fuzzy set.

3) *Defuzzification:* The output fuzzy set is converted to a crisp value by applying the preferred defuzzification method, such as the center of gravity (CoG) approach reported in [37].

This workflow is graphically reported in Fig. 1. The QFIE proposed in [5] replaces the FIE resulting in a speedup in the computational time of the overall FRBS that is due to two main factors: first, thanks to the intrinsic parallelism of quantum computing, the evaluation of the *antecedents* is executed in parallel and no longer as in the classical case sequentially; second, in the QFIE, the *implication* and *aggregation* operations depend on the number of linguistic terms defined for the output variable in the FRBS and no longer on its number of rules, which is generally much higher. These features of QFIE stem from an innovative amplitude encoding of fuzzified values in quantum states and a formalization of the fuzzy rule set as a Boolean oracle that can be easily implemented in terms of quantum gates. Hereafter, this aspect will be briefly analyzed, while a more rigorous mathematical description can be found in [5].

The QFIE is implemented by considering for each input fuzzy variable $X_j = \{T_{1j}, T_{2j}, \ldots, T_{m_j j}\}$ and for the related crisp input x_j a quantum register composed of $\eta_j = \lceil \log_2(|X_j|) \rceil$ qubits initialized as

$$|\psi_j\rangle = \sum_{i=1}^{m_j} \sqrt{\alpha_{ij}} |T_{ij}\rangle \tag{6}$$

where α_{ij} is the membership degree of x_j to T_{ij}, and by abuse of notation, T_{ij} is being understood as an η_j-dimensional Boolean string. The only constraint for this initialization is that $\sum_{i=1}^{m_j} \alpha_{ij} \leq 1$. Moreover, a dummy linguistic term can be added to ensure the normalization in (6) if required. By iterating this initialization procedure for all the input variables, the resulting quantum state can be written as the tensor product of the individual states $\{|\psi_j\rangle\}_{j=1}^{n}$:

$$|\psi_1, \psi_2, \ldots \psi_n\rangle = \sum_{i=1}^{m_1} \sum_{t=1}^{m_2} \cdots \sum_{r=1}^{m_n} \sqrt{\alpha_{i1} \cdot \alpha_{t2} \cdot \ldots \cdot \alpha_{rn}} |T_{i1}, T_{t2}, \ldots, T_{rn}\rangle. \tag{7}$$

This state contains as basis states all the possible antecedents having the form given in (5), and each square amplitude is its fire strength computed by the product T-norm [38]. By using a more compact notation, we have

$$|\psi_1, \psi_2, \ldots \psi_n\rangle = \sum_{a \in \mathcal{A}_s} \sqrt{F_a} |a\rangle \tag{8}$$

where $\mathcal{A}_s$ is the set of all the possible antecedents denoted as a concatenation of Boolean strings. At this point, supposing that the output variable of the FRBS $Y = \{T_{1Y}, T_{2Y}, \ldots, T_{m_Y Y}\}$ is composed of m_Y linguistic terms, the quantum state in (8) is used by the QFIE as the input state for a Boolean quantum oracle O_f implementing the following operation:

$$|\psi_Y\rangle = \mathcal{O}_f |\psi_1, \psi_2, \ldots, \psi_n\rangle |\bar{0}\rangle = \sum_{i=1}^{m_Y} \sum_{a \in \mathcal{A}_S^i} \left(\sqrt{F_a} |a\rangle |c_i\rangle \right) + \sum_{a \in \mathcal{A}_S^0} \left(\sqrt{F_a} |a\rangle |\bar{0}\rangle \right) \tag{9}$$

where $\bar{0}$ is an m_Y-dimensional Boolean string composed of all zeros and c_i indicates the linguistic term T_{iY} as a Boolean string with all zeros and a single one at the ith bit. In (9), $\mathcal{A}_S^i$ indicates the set of all the antecedents having T_{iY} as consequent in a fuzzy rule and $\mathcal{A}_S^0$ indicates the set of all the antecedents that do not have a consequent specified in the FRBS rule set. Equation (9) states that by just one query to the quantum oracle O_f using as input the superposed quantum state containing all the possible antecedents (8), it is possible to create an entangled state with the corresponding consequent where the squared amplitude of each basis state is related to the strength of the rule that such basis state represents. At this point, the final output fuzzy set can be obtained by measuring the output quantum state in $|\psi_Y\rangle$ several times in such a way as to retrieve the probability of measuring each $|c_i\rangle$ state, with $i = 1, \ldots, m_Y$. Indeed, it is easy to show that

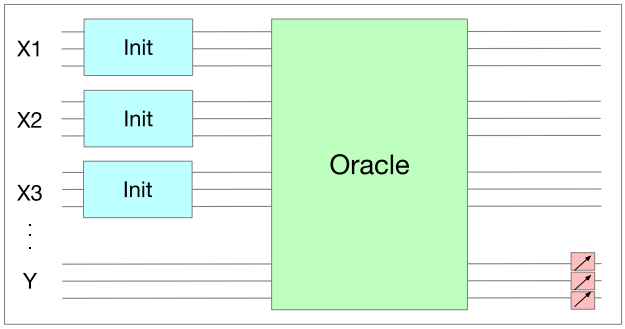

FIGURE 2. High-level view of a quantum circuit implementing QFIE.

[1]The fuzzy preposition after "THEN" is denoted as *consequent*.

IEEE Transactions on Quantum Engineering

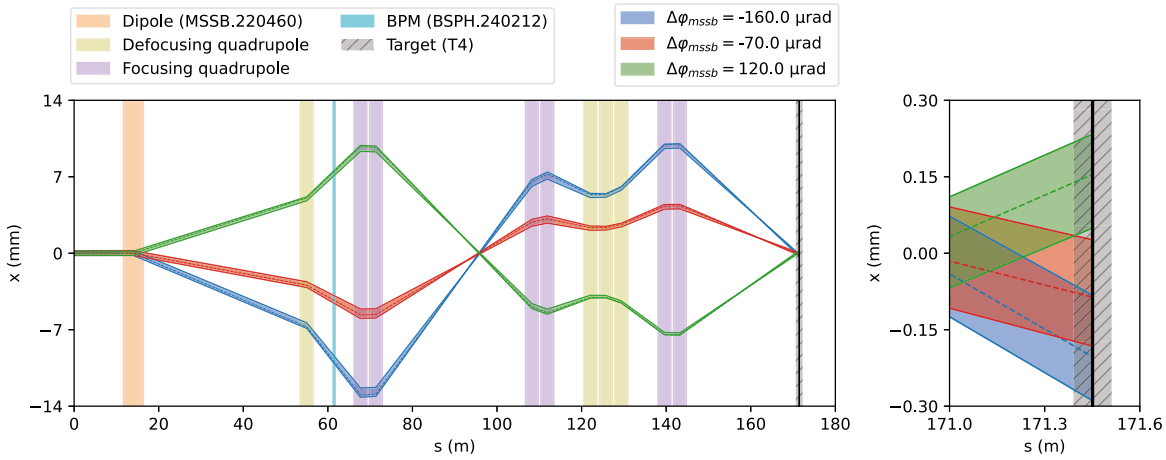

FIGURE 3. One-dimensional beam target steering task at the CERN TT24-T4 beamline. (Left) Horizontal beam trajectories obtained from tracking simulations are shown for three different settings of the main deflecting dipole (orange). (Right) Zoomed view on the target (gray, hatched) region showing the horizontal position of impact of the beam for the three settings of the main dipole [39].

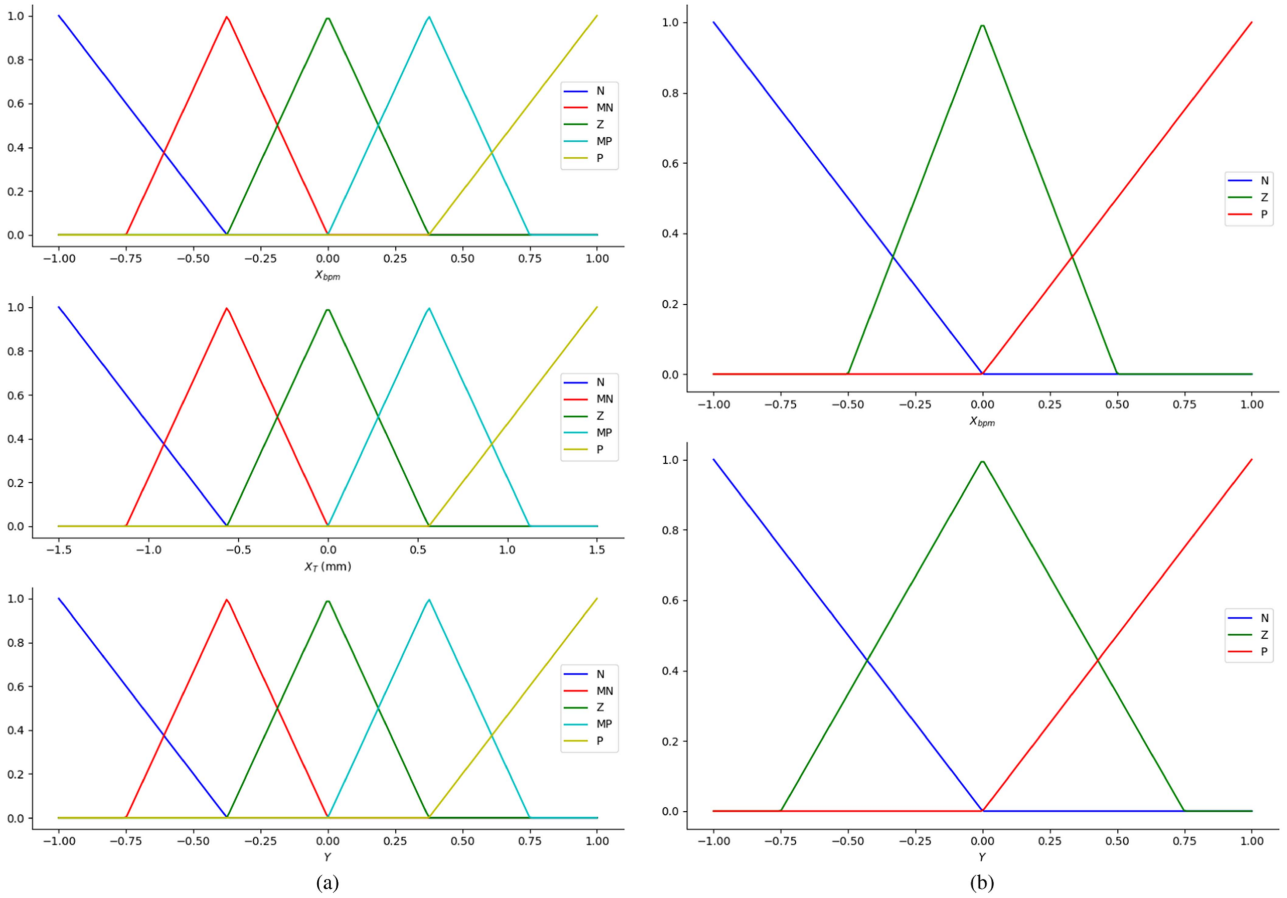

FIGURE 4. Membership functions for (a) C1 and (b) C2.

the probability of measuring c_i is

$$P_{c_i} = \sum_{a \in \mathcal{A}_S^i} F_a \quad \forall i \in [1, m_Y]\,. \tag{10}$$

Starting from these probabilities, the output fuzzy set is obtained by cutting the fuzzy set related to the linguistic term T_{iY} at the value P_{c_i} $\forall\ i \in [1, m_Y]$. Finally, a classic defuzzification approach is used to retrieve the final crisp output. Fig. 2 represents a schematic view of the quantum circuit implementing QFIE.

From a computational point of view, a classical FRBS performs m^n queries to the oracle, that is the number of fuzzy

X_{bpm}

X_T \	N	MN	Z	MP	P
N	Z	MN	N	N	N
MN	MP	Z	MN	N	N
Z	MP	MP	Z	MN	MN
MP	P	P	MP	Z	MN
P	P	P	P	MP	Z

(a)

X_{bpm}

N	Z	P
P	Z	N

(b)

FIGURE 5. Rule set for (a) C1 and (b) C2. The conjunction of the elements of the first row and column represents the antecedent part of a fuzzy rule having as consequent the corresponding matrix element. For instance, the first rule in C1 corresponds to the sentence If X_{bpm} is negative and X_T is negative, then the correction angle is zero.

rules in a complete set of rules where it is supposed that all the input fuzzy variables have the same number of fuzzy sets m, i.e., $m_j = m \, \forall j \in [1, n]$. On the other hand, a QFIE-based FRBS performs only one query to the oracle to evaluate all the rules simultaneously. However, to reconstruct the distribution of probability in (10), N_s shots are required, i.e., the quantum circuit implementing the oracle is executed for N_s times. As discussed in [5], N_s can be related to the fidelity level F at which the probability distribution is reconstructed and to the number of possible outcomes of the circuit, which is equal to 2^{m_y}, by using the following relationship:

$$N_s \approx \frac{2^{m_y}}{(1-F)^2}. \tag{11}$$

Therefore, the QFIE performs a lower number of queries to the oracle than the classical counterpart when

$$\frac{2^{m_y}}{(1-F)^2} < m^n. \tag{12}$$

As an example, considering a typical number of fuzzy sets $m_y = m = 5$ and a level of fidelity $F = 0.95$, the quantum advantage is reached once the number of input variables is higher than $n = 6$.

IV. QFIE FOR PARTICLE ACCELERATOR CONTROL

The goal of this work is to address various control issues that arise in the CERN accelerator complex by using the QFIE. Two beamlines from the complex are examined to investigate different levels of complexity in control problems. The first task involves directing a proton beam toward a target with a single control variable, while the second one aims at correcting the beam trajectory of the AWAKE electron line employing ten control parameters. The project primarily utilizes accurate simulations of these beamlines to develop and test the implementation of QFIE for control purposes. The environments for these simulations are constructed using the OpenAI GYM template [40]. Successively, as reported in Section V, the QFIE-based FRBS was employed to control in real time the actual AWAKE electron beamline. In all the tests, QFIE implementation is carried out through the Python package available on GitHub.[2]

A. TARGET STEERING ENVIRONMENT CONTROL

This section aims to show the application of QFIE in controlling the 1-D beam target steering environment based on the beam optics of the TT24-T4 transfer line at CERN [6]. This line is about 170 m long and transports protons with a momentum of 400 GeV/c from the SPS to some of the fixed-target physics experiments installed in the CERN North Area. TT24 is equipped with several dipole and quadrupole magnets to steer and focus the beam, beam position monitors (BPMs) to measure the beam centroid at various places along the line, drift spaces, and the actual target placed at the end of the line. The objective of the task is to optimize the number of particles hitting the target by tuning the first dipole magnet in the line to maximize the event rates in the particle detectors. The left-hand side of Fig. 3 shows the relevant elements of TT24 together with horizontal beam trajectories obtained from tracking simulations for three different settings of the main bending dipole. Depending on the dipole deflection angle, the particles hit the target (gray, hatched) at different horizontal positions, as illustrated by the zoomed view on the right-hand side of the figure. There are focusing (purple) and defocusing (olive) quadrupoles along the beamline to keep the beam particles confined. The terms "focusing" and "defocusing" refer to the effect of the quadrupole magnets on the particle beam in the horizontal plane. Their impact is inverse in the vertical plane.

Overall, the QFIE-based controller implemented aims to deflect the beam via controlling the 1-D deflection angle Y of the main magnetic dipole (see Fig. 3, orange) according to two input variables such as the position reading of one of the BPMs installed in the beamline (cyan) X_{bpm} and the desired target position X_T. The allowed range of deflection angles is $[-140, 140]$ μrad.

Two scenarios have been considered: in the first configuration (C1), X_T was any value in the range $[-1.5, 1.5]$ mm, while in the second configuration (C2), X_T was set to zero, and therefore, X_{bpm} was the only input variable of the system. This simplification of the environment enables the construction of smaller quantum circuits for the QFIE that can be reliably executed on real quantum hardware. Finally, to assess how well the beam is hitting the target, the following reward function is considered:

$$\mathcal{R} = -(1 - I) \tag{13}$$

where I represents the intensity of the Gaussian beam in the range $X_T \pm 3\sigma$. I is normalized to the total intensity (number

[2]https://github.com/Quasar-UniNA/QFIE

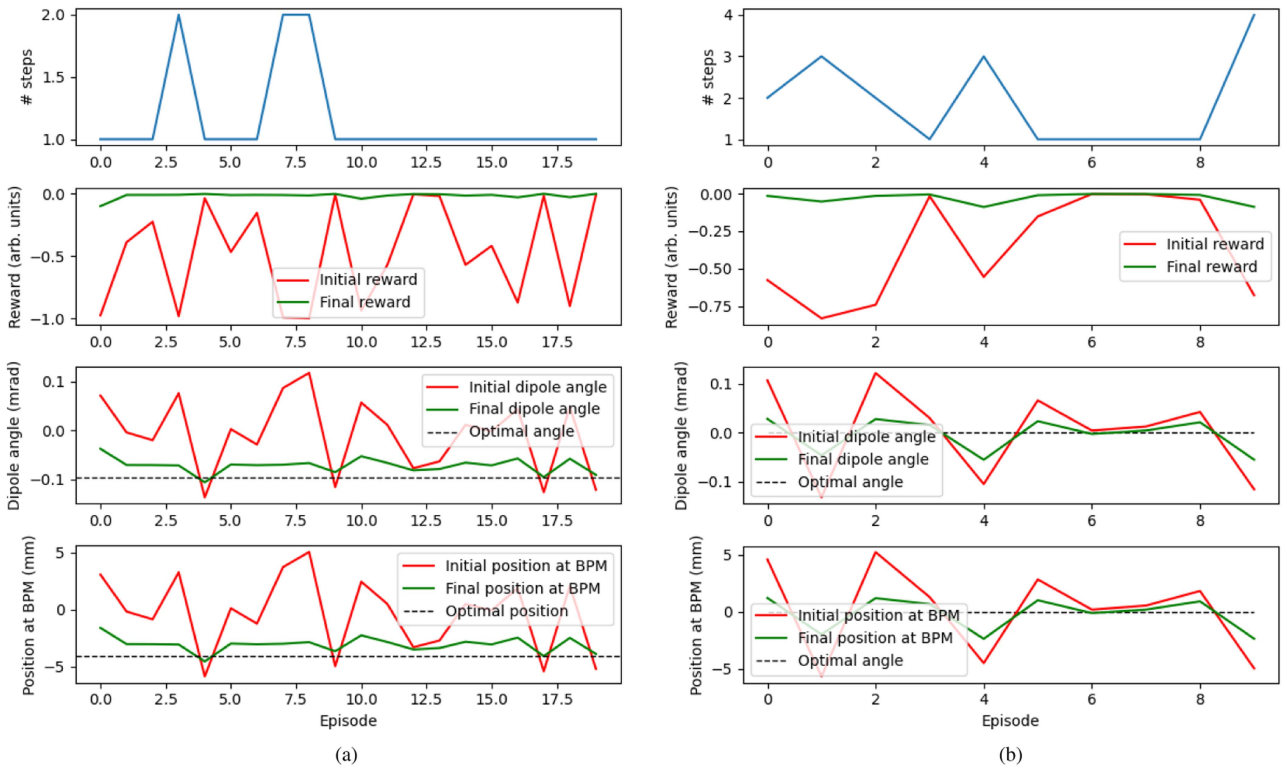

FIGURE 6. Experimental results for the target steering environment control by computing QFIE quantum circuits (a) via noiseless simulation C1 and (b) via execution on IBMQ Montreal quantum processor C2. For each configuration, it is reported for all the episodes the number of steps, the initial and final reward value, dipole angle, and position of the beam measured at the BPM.

of protons) extracted from the SPS and $\sigma = 6.0$ mm denotes the horizontal beam size at the target assuming a fixed geometric horizontal emittance of 11.8 nm · rad and given the horizontal beta function of 7.1 m. The beam is hitting the perfect target position when $\mathcal{R} = 0$.

The fuzzy partitions and the rule base used by the QFIE in controlling C1 and C2 are reported in Figs. 4 and 5, respectively. These configurations of the FRBS have been derived empirically. For C1, five linguistic terms were considered for each variable: negative (N), medium negative (MN), zero (Z), medium positive (MP), and positive (P). As a consequence, the number of fuzzy rules having as antecedent an *and* connection of two linguistic terms related to the different input variables is 25. For C2, three linguistic terms were considered for the input and the output variable: negative (N), zero (Z), and positive (P). This leads to a set of three fuzzy rules. The limited number of fuzzy rules in C2 enables the execution of QFIE also on real NISQ devices, while their high level of noise forces the control of C1 via noiseless simulations of QFIE. In detail, on the IBMQ Montreal quantum processor, the transpiled[3] quantum circuit implementing QFIE for C1 control has a depth of 3182 with 1554 CNOT gates, while the transpiled quantum circuit of QFIE for C2 control has an overall depth of 42 and a number of CNOTs equal to 20.

[3]Transpilation is the process by which a quantum circuit is decomposed into basic gates for being executed on a specific quantum hardware. More details can be found in [41].

1) EXPERIMENTAL RESULTS

For C1 evaluation, 20 different episodes with different initial beam positions were considered, while the target X_T was randomly selected in the range $[-1.5, 1.5]$ mm. Both X_{bpm} and Y have been normalized in the simulations in the range $[-1, 1]$. For the sake of space, the reported results refer just to a particular target position, but the performances are very similar for all the different target positions tested. For C2 evaluation, due to the limitation in time for the availability of IBM quantum devices, just ten different initial beam positions were considered. In particular, these experiments have been carried out on the IBMQ Montreal device. In each episode and for both C1 and C2, the controller deflects the beam until a threshold reward value of -0.1 is reached. The results obtained for both C1 and C2 are reported in Fig. 6(a) and (b), respectively. In detail, the upper plots represent the number of controller actions (steps) required to achieve the reward threshold. The second plot reports the value of the reward function $\mathcal{R}$ at the beginning of the episode (red line) and at the end of it (green line). The two boxes on the bottom of the figure represent the dipole angle in mrad (Y) and the beam position at the BPM in millimeters, respectively. The dashed lines represent the ideal output of the system, while the red and green lines show the initial and final values, respectively. For configuration C2, the ideal output for both these plots is 0, where the target was set. It can be seen that the QFIE is able to control the environment in all the episodes and for both configurations. The absence of noise

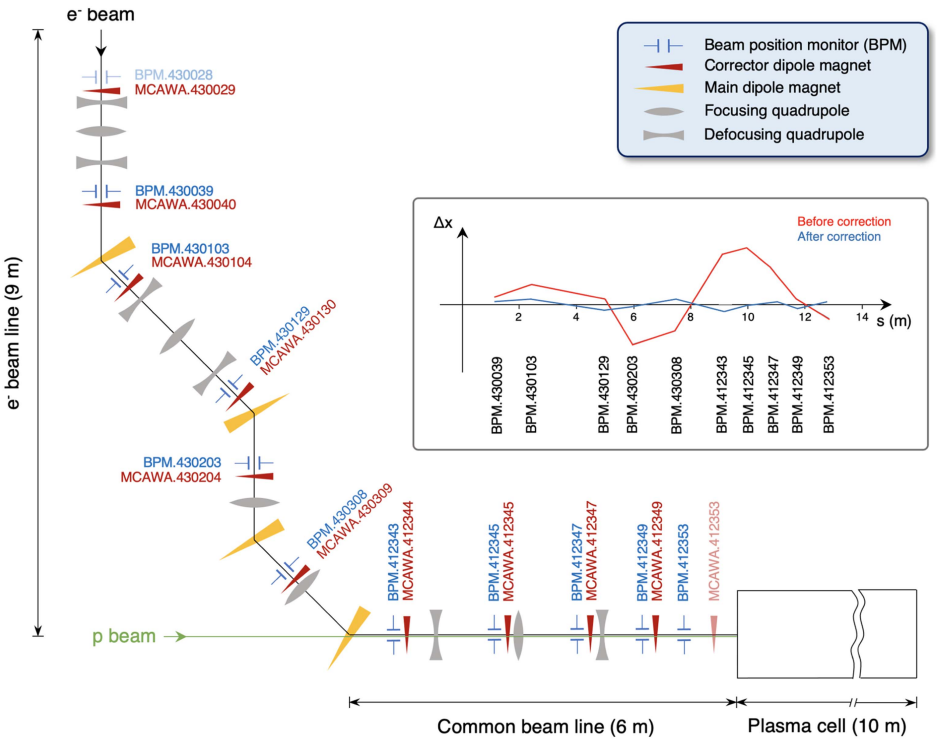

FIGURE 7. Representation of the CERN AWAKE electron beamline with (red) ten trajectory correctors and (blue) ten BPMs per plane. The inset shows electron beam trajectories (red) before and (blue) after correction, respectively.

during the simulation for C1 enables the control of the beam with two steps at worst. On the other hand, the noise in computing the QFIE action that occurs in C2 and the lower granularity of the input fuzzy partition make more steps required for achieving the optimal solution. Overall, these results prove the suitability of QFIE in controlling this kind of environment, both by means of simulations of the quantum circuits and by means of execution on real quantum hardware.

B. ELECTRON BEAMLINE CONTROL

The AWAKE at CERN uses high-intensity 400-GeV proton bunches from the SPS as a plasma wakefield driver [42]. Electron bunches are simultaneously steered into the plasma cell to be accelerated by the proton-induced wakefields. In the AWAKE Run 1 (2016–2018), electron energies up to 2 GeV have been demonstrated over a plasma cell of 10-m length corresponding to an electric field gradient of 200 MV/m [43]. The goals of the currently ongoing Run 2 are to demonstrate stable field gradients of up to 1 GV/m and emittance preservation of the electron bunches, and to develop plasma sources scalable to 100s meters and beyond. Ultimately, by the end of Run 2, the AWAKE scheme should start providing electron bunches for particle physics experiments [44]. The targeted field gradients are to be compared to conventional accelerating structures using radio frequency (rf) cavities in the X-band regime, which are currently limited to about 150 MV/m [45]. The AWAKE electron source and electron beamline are particularly interesting for algorithm preparation and testing due to the high repetition rate and insignificant damage potential in case of losing the beam at accelerator components. The AWAKE electrons are generated in a 5.5-MV photocathode rf gun, accelerated to 16 MeV and then transported through a beamline of 12 m to the AWAKE plasma cell [7]. The electron line is equipped with 12 BPMs and 12 steering dipoles per plane, respectively, of which ten horizontal correctors and subsequent BPMs are used for the steering task. The BPM electronic read-out is at 10 Hz and acquisition through the CERN middleware is at 1 Hz. Fig. 7 shows the electron beamline, extending from the electron source (top left) to the entrance of the plasma cell (bottom right). The schematic includes horizontally focusing and defocusing quadrupoles (gray), main dipoles (yellow) that steer the beam, BPMs (blue) for tracking beam position, and corrector dipoles (red) for beam trajectory adjustments. The inset plot illustrates two potential horizontal electron beam paths by showing the horizontal displacement of the beam's center of mass from the central magnetic axis at each BPM location, marked at distance s from the electron source. The red and blue curves depict the beam trajectories before and after correction, respectively. The goal was to develop a QFIE-based controller able to correct the horizontal trajectory with similar accuracy as the response-matrix-based singular value decomposition algorithm that has traditionally been used [46].

The input state of the controller is formalized as a 10-D vector of horizontal beam position measured with respect to the reference trajectory. Accordingly, the controller action is a 10-D vector of the horizontal corrector dipole magnet kick

IEEE Transactions on Quantum Engineering

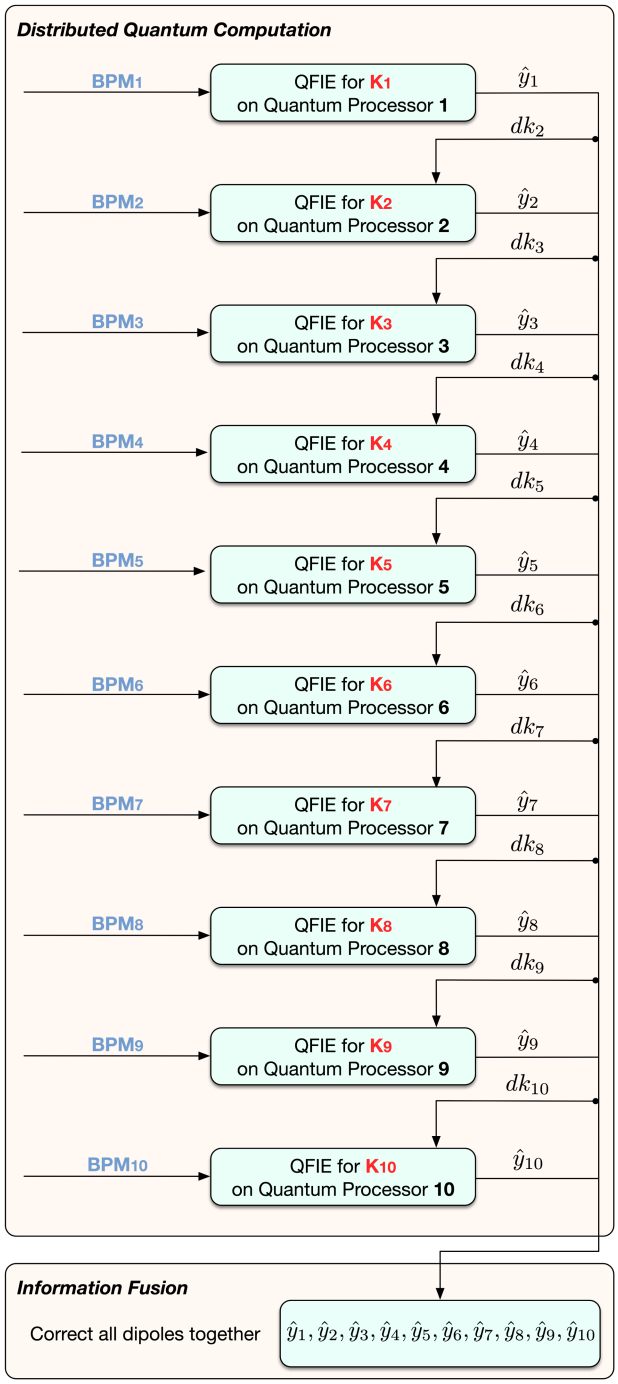

FIGURE 8. D-NISQ computation of the quantum FRBS for the AWAKE beamline.

angles within a range of ± 300 μrad. To evaluate the performance of the controller, a reward function is used that consists of the negative root mean square (rms) of the measured beam trajectory with respect to the reference at all the BPMs.

Developing a single QFIE controlling simultaneously all the corrector dipole magnets along the AWAKE trajectory would reflect in a quantum circuit too big for being classically simulated or executed on a current NISQ device. Therefore, to solve the control problem, an approach based on the D-NISQ reference model proposed in [32] has been exploited: the original 10-D problem was divided into ten 1-D control problems, where each corrector dipole magnet K_i with $i \in [1, 10]$ is controlled by a QFIE, QFIE_i with $i \in [1, 10]$. Each QFIE_i $\forall i \in [2, 10]$ acts considering two input variables x_i and dk_i, where the former refers to the distance from the ideal position of the beam registered by the corresponding BPM_i, while the latter refers to the sum of the normalized deviation carried out by the magnets that are placed previously to the ith magnet on the AWAKE beamline. Formally, denoting with $\hat{y}_i$ the corrector dipole magnet kick angles computed by QFIE_i, the dk_m input variable for QFIE_m is defined as follows:

$$dk_m = \sum_{i=1}^{m-1} \hat{y}_i. \tag{14}$$

The action of QFIE_1 depends just on the position of the particle beam at the first BPM along the trajectory. In detail, dk_i is defined in an interval $[-2,2]$ $\forall i \in [2, 10]$, x_i is defined in an interval $[-1,1]$ $\forall i \in [1, 10]$, and the output corrector dipole magnet kick angles y_i are defined in the normalized interval $[-1,1]$ $\forall i \in [1, 10]$.

Fig. 8 summarizes graphically how the whole FRBS has been distributed according to the D-NISQ architecture. However, due to the quantum noise affecting current quantum processors, the quantum circuits implementing the different QFIE_i $\forall i \in [1, 10]$ were ideally simulated.

The fuzzy partitions used for the variables of each QFIE_i are the same. In particular, Fig. 9 shows them for QFIE_{10}. Moreover, Fig. 10(a) shows the fuzzy rule base for QFIE_i $\forall i \in [2, 10]$, while Fig. 10(b) shows the fuzzy rule base for QFIE_1. This configuration for each FRBS has been established empirically.

To minimize the number of interactions of the whole controller with the environment, a bias factor b has been multiplied by the ten QFIEs' output. Formally, denoting with $\hat{y}_i$ the output computed by QFIE_i, the final corrector dipole magnet kick angle y_i used to modify the environment state is obtained as follows:

$$y_i = \begin{cases} \hat{y}_i \cdot b, & \text{if } \hat{y}_i \cdot b \in [-1, 1] \\ 1, & \text{if } \hat{y}_i \cdot b > 1 \\ -1, & \text{if } \hat{y}_i \cdot b < -1. \end{cases} \tag{15}$$

In our experiments, b has been set to 10 empirically.

1) EXPERIMENTAL RESULTS

Fig. 11 reports the experimental results obtained by simulating the AWAKE environment controlled by QFIEs. The simulations stop when the reward objective reaches an rms value of better than or equal to 2 mm. As shown by the plots, considering 50 different episodes, where the initial condition of the beam is far away from the threshold rms value, the quantum fuzzy control system is able to align the particle beam to the ideal trajectory in 100% of the episodes. Moreover, in all the episodes, the desired trajectory is obtained at the worst by means of two interactions of the controllers

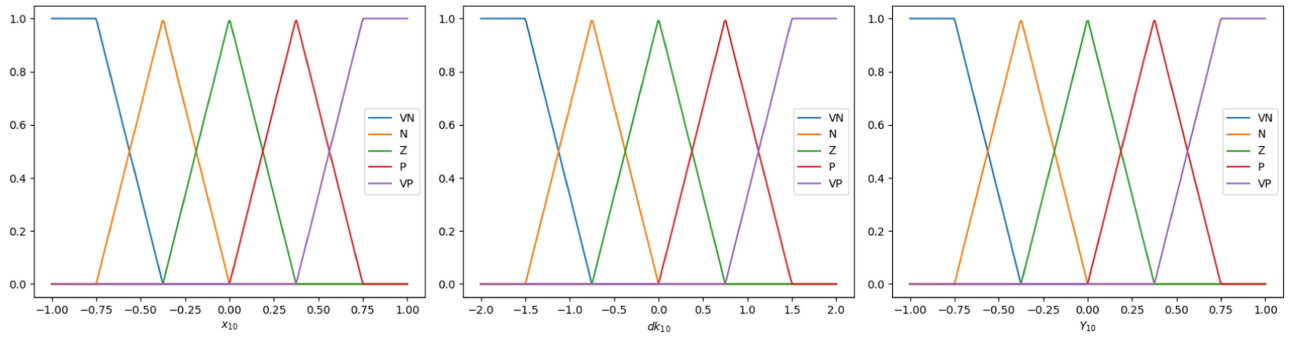

(a) (b) (c)

FIGURE 9. Fuzzy partitions for $QFIE_{10}$ (a), (b) input, and (c) output variables.

dk_i

x_i	VN	N	Z	P	VP
VN	VP	VP	VP	P	Z
N	VP	VP	P	Z	N
Z	VP	P	Z	N	VN
P	P	Z	N	VN	VN
VP	Z	N	VN	VN	VN

(a)

x_1

VN	N	Z	P	VP
VP	P	Z	N	VN

(b)

FIGURE 10. Rule set for (a) $QFIE_i$ $\forall i \in [2, 10]$ and (b) $QFIE_1$. The conjunction of the elements of the first row and column represents the antecedent part of a fuzzy rule having as consequent the corresponding matrix element. For instance, the first rule in $QFIE_i$ corresponds to the sentence If dk_i is very negative and x_i is very negative then the correction angle is very positive.

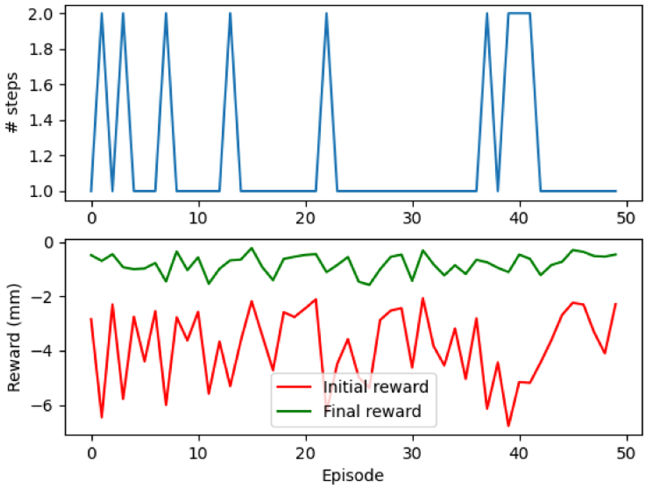

FIGURE 11. Experimental results on the simulated AWAKE environment. For each episode, (top) the number of controller iterations and (bottom) the initial and final reward values are reported.

with the environment, proving the sample efficiency of the proposed quantum controller also in this case study.

V. ONLINE TESTS ON REAL AWAKE ENVIRONMENT

The QFIE-based FRBS was also evaluated on the real AWAKE environment to test sim-to-real transfer. The same configuration of QFIE considered for the simulated environment has been exploited. In detail, the distributed approach used to compute the 10-D action enables a fast simulation time of the circuits, which made it possible to test the proposed approach in real time on the actual AWAKE facility. In this scenario, the input x_i used by each $QFIE_i$ is the actual reading of the related BPM along the AWAKE beamline averaged over ten consecutive acquisitions to reduce the shot-to-shot variation. Given the inputs, sequentially, all the quantum circuits implementing the different QFIEs are simulated, and from each of them, the kick angles for the related dipole magnet on the trajectory are retrieved. Once the ten kick angles have been obtained, the trajectory correctors along the AWAKE beamline simultaneously modify the electron beam trajectory. At this point, by using the new BPM readings, the rms distance with respect to the ideal trajectory is computed, and if this value is above a certain threshold, the QFIE-based fuzzy controller performs another operation on the beamline changing again the magnet kick angles. The fuzzy controller stops when the rms value is under a given reward objective threshold value. In our tests, we performed four different sets of experiments considering four different levels of rms thresholds: 2, 1.6, 1.2, and 0.8 mm, respectively. A lower absolute reward value reflects in a more precise control of the particle beam. Moreover, for each set of experiments, 20 independent episodes were collected, i.e., the trajectory correctors on the AWAKE beamline were randomly initialized 20 times. Fig. 12 shows the histograms reporting the obtained results for all the different levels of reward objective threshold value, −2 mm [see Fig. 12(a)], −1.6 mm [see Fig. 12(b)], −1.2 mm [see Fig. 12(c)], and −0.8 mm [see Fig. 12(d)]. In detail, histograms in Fig. 12 report the distribution of the number of times in which the fuzzy controller has modified the trajectory correctors (#Steps), i.e., the number of interactions environment control required to reach the

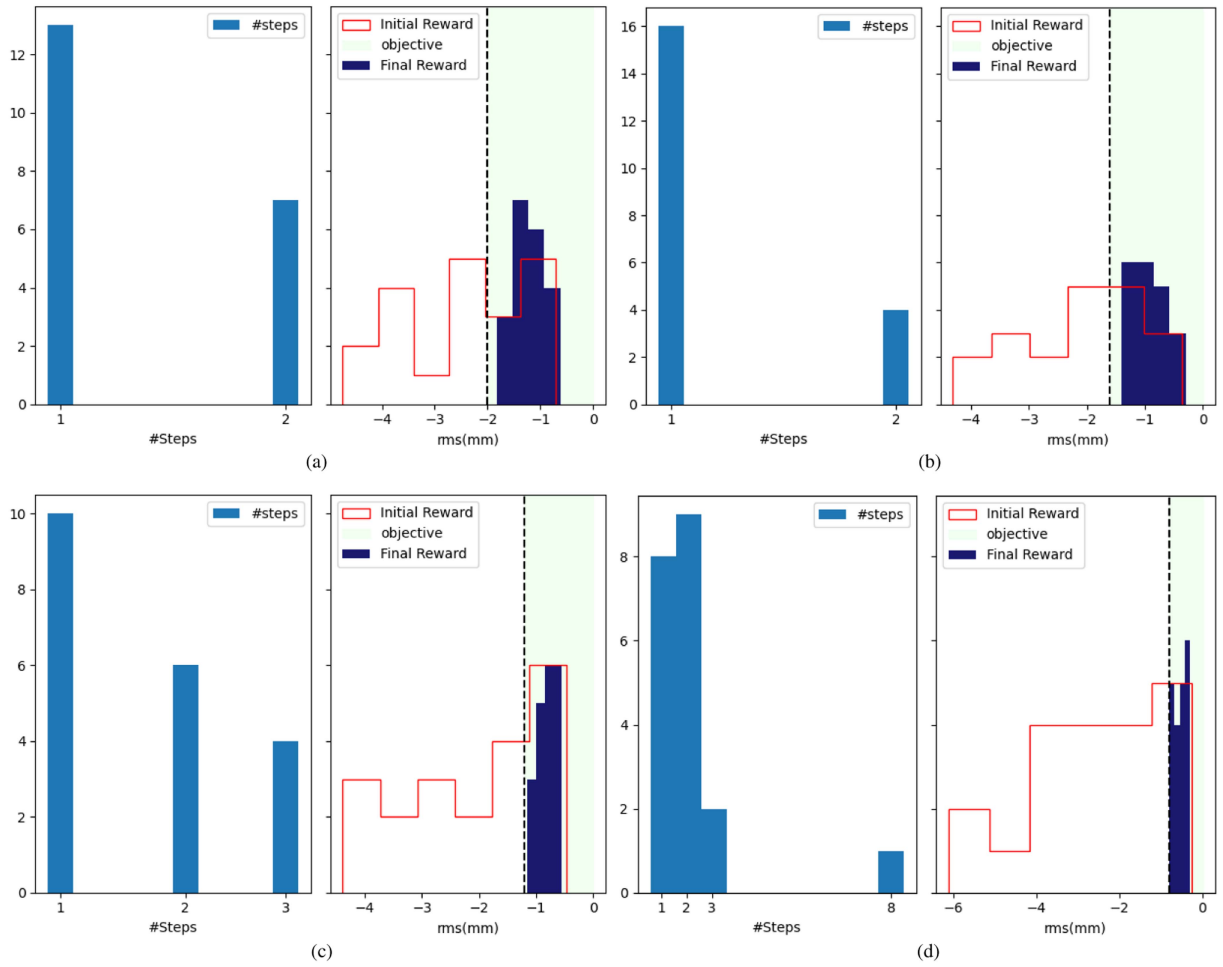

FIGURE 12. **Online experiments on the real AWAKE beamline. The figure displays the same plots for the four different values of rms threshold set in the experiments [2, 1.6, 1.2, and 0.8 mm, respectively, reported in (a)–(d)]. In each configuration, both the distribution of the number of steps required to achieve the related rms threshold value (on the left) and the distribution of the initial and the final rms values (on the right) are reported. The dashed lines represent the rms threshold values. For all the different rms thresholds, 20 independent episodes have been carried out. (a) rms = 2 mm. (b) rms = 1.6 mm. (b) rms = 1.6 mm. (d) rms = 0.8 mm.**

desired rms value, and the distribution of the 20 initial state reward values (i.e., the rms distance from the ideal trajectory at the beginning of an episode), and the distribution of the 20 final state reward values (i.e., the rms distance from the ideal trajectory at the end of an episode). As highlighted by the plots, the QFIE-based controller is able to solve the control problem also in the real AWAKE environment. Indeed, the objective reward value is reached in 100% of the episodes considered. The number of steps required to achieve such an impressive result is in line with the simulated environment, except for an outlier in the scenario with an rms threshold equal to 0.8 mm.

VI. CONCLUSION

In this article, a QFIE-based FRBS [5] has been experimentally tested for the very first time to control real-world environments, such as those related to particle physics accelerators at CERN facilities. The main result obtained from this research is twofold: on the one hand, it has been shown that the QFIE is able to control these complex environments by means of simulations and real executions of quantum circuits implementing the algorithm on a quantum computer; on the other hand, it has been proved that quantum FRBSs could be a valid tool for the real-time control of particle accelerators for the physics experiments at CERN, as shown by the test carried out on the real AWAKE beamline.

In detail, research was carried out on two successive scenarios, two existing CERN beamlines representing control problems of different degrees of complexity. In the first scenario, the QFIE controller implemented aims to deflect the beam via the magnetic dipole in an environment based on the TT24-T4 transfer line at CERN: in this simpler context, the whole algorithm was also executed on a real IBM Quantum computer, proving the feasibility of QFIE in controlling this kind of environment on real quantum devices. The second scenario consists of the AWAKE use case, where the 10-D environment is much more complex and current NISQ devices are not ready to handle the resulting QFIE circuits. However, in this case, the simulated quantum circuits were

tested on real data as an online controller of the beamline. This result proves for the very first time the capability of an FRBS to control a real particle accelerator.

In the future, the QFIE-based FRBS will be developed and tested for more complex experiments and environments, where no analytical solutions are available to control the systems. In these cases, where the number of variables to control makes the empiric development of fuzzy rules impractical, as done for the experiments carried out in this first study, QFIE-based FRBSs can be integrated with automatic techniques to learn fuzzy rules and fuzzy partitions from data [47], [48]. By doing that, the number of fuzzy rules can explode exponentially due to the fuzzy rule explosion problem, making a classical FRBS unfeasible to efficiently control a particle accelerator. However, QFIE-based FRBSs are exponentially faster in performing fuzzy inference than the classical equivalent, and therefore, they are the perfect candidate to counter the fuzzy rule explosion problem, opening a completely new era for particle accelerator control systems. Yet, the size of the quantum circuits implementing QFIE when the number of rules to execute is big makes the simulation of QFIE impractical for classical simulators, and real fault-tolerant quantum computers are required to achieve the goal. Considering this, while the next generation of quantum computers will be ready, quantum error mitigation techniques will be exploited to reduce the effect of quantum noise on the QFIE also in the NISQ era.

ACKNOWLEDGMENT

The authors thank the Beams Department and the Advanced Proton Driven Plasma Wakefield Acceleration Experiment collaboration at the European Organization for Nuclear Research (CERN) for their availability and support. The authors would also like to thank the ATLAS collaboration at CERN.

REFERENCES

[1] L. A. Zadeh, "Fuzzy sets," *Inf. Control*, vol. 12, pp. 94–102, 1968, doi: 10.1016/S0019-9958(68)90211-8.

[2] L. A. Zadeh, "Fuzzy sets," in *Fuzzy Sets, Fuzzy logic, and Fuzzy Systems*. Singapore: World Scientific, 1996, pp. 394–432, doi: 10.1142/2895.

[3] M. Sugeno, "An introductory survey of fuzzy control," *Inf. Sci.*, vol. 36, nos. 1/2, pp. 59–83, 1985, doi: 10.1016/0020-0255(85)90021-0.

[4] R.-E. Precup and H. Hellendoorn, "A survey on industrial applications of fuzzy control," *Comput. Ind.*, vol. 62, no. 3, pp. 213–226, 2011, doi: 10.1016/j.compind.2010.10.001.

[5] G. Acampora, R. Schiattarella, and A. Vitiello, "On the implementation of fuzzy inference engines on quantum computers," *IEEE Trans. Fuzzy Syst.*, vol. 31, no. 5, pp. 1419–1433, May 2023, doi: 10.1109/TFUZZ.2022.3202348.

[6] G. L. D'Alessandro et al., "Target bypass beam optics for future high intensity fixed target experiments in the CERN north area," in *Proc. Int. Part. Accel. Conf.*, pp. 3046–3048, 2021, doi: 10.18429/JACoW-IPAC2021-WEPAB185.

[7] K. Pepitone et al., "The electron accelerators for the AWAKE experiment at CERN—Baseline and future developments," *Nucl. Instrum. Methods Phys. Res. Sec. A: Accel., Spectrometers, Detectors Assoc. Equip.*, vol. 909, pp. 102–106, 2018, doi: 10.1016/j.nima.2018.02.044.

[8] J. Preskill, "Quantum computing in the NISQ era and beyond," *Quantum*, vol. 2, 2018, Art. no. 79, doi: 10.22331/q-2018-08-06-79.

[9] A. Abbas, D. Sutter, C. Zoufal, A. Lucchi, A. Figalli, and S. Woerner, "The power of quantum neural networks," *Nature Comput. Sci.*, vol. 1, no. 6, pp. 403–409, 2021, doi: 10.1038/s43588-021-00084-1.

[10] F. Tacchino, C. Macchiavello, D. Gerace, and D. Bajoni, "An artificial neuron implemented on an actual quantum processor," *npj Quantum Inf.*, vol. 5, no. 1, pp. 1–8, 2019, doi: 10.1038/s41534-019-0140-4.

[11] B. Doolittle, R. T. Bromley, N. Killoran, and E. Chitambar, "Variational quantum optimization of nonlocality in noisy quantum networks," *IEEE Trans. Quantum Eng.*, vol. 4, 2023, Art. no. 4100127, doi: 10.1109/TQE.2023.3243849.

[12] G. Acampora, R. Schiattarella, and A. Vitiello, "Using quantum amplitude amplification in genetic algorithms," *Expert Syst. Appl.*, vol. 209, 2022, Art. no. 118203, doi: 10.1016/j.eswa.2022.118203.

[13] G. Acampora and A. Vitiello, "Implementing evolutionary optimization on actual quantum processors," *Inf. Sci.*, vol. 575, pp. 542–562, 2021, doi: 10.1016/j.ins.2021.06.049.

[14] Y.-P. Huang, P. Singh, W.-L. Kuo, and H.-C. Chu, "A type-2 fuzzy clustering and quantum optimization approach for crops image segmentation," *Int. J. Fuzzy Syst.*, vol. 23, no. 3, pp. 615–629, 2021, doi: 10.1007/s40815-020-01009-2.

[15] J. Li and Z. Hao, "A quantum probabilistic linguistic term framework to multi-attribute decision-making for battlefield situation assessment," *Int. J. Fuzzy Syst.*, vol. 24, no. 1, pp. 495–507, 2022, doi: 10.1007/s40815-021-01151-5.

[16] M. Hou, S. Zhang, and J. Xia, "Quantum fuzzy k-means algorithm based on fuzzy theory," in *Proc. Int. Conf. Adaptive Intell. Syst.*, 2022, pp. 348–356, doi: 10.1007/978-3-031-06794-5_28.

[17] S. Ishikawa and K. Kikuchi, "Quantum fuzzy logic and time," *J. Appl. Math. Phys.*, vol. 9, no. 11, pp. 2609–2622, 2021, doi: 10.4236/jamp.2021.911168 .

[18] R. Leporini, C. Bertini, and F. C. Fabiani, "Fuzzy representation of finite-valued quantum gates," *Soft Comput.*, vol. 24, no. 14, pp. 10305–10313, 2020, doi: 10.1007/s00500-020-04870-3.

[19] D. Aerts, T. Durt, and B. Van Bogaert, "A physical example of quantum fuzzy sets and the classical limit," *Tatra Mountains Math. Publ.*, vol. 1, pp. 5–15, 1993.

[20] J.-T. Yan, "Fuzzy-based balanced partitioning under capacity and size-tolerance constraints in distributed quantum circuits," *IEEE Trans. Quantum Eng.*, vol. 4, 2023, Art. no. 5100115, doi: 10.1109/TQE.2023.3272023.

[21] G. Acampora and A. Vitiello, "Error mitigation in quantum measurement through fuzzy C-means clustering," in *Proc. IEEE Int. Conf. Fuzzy Syst.*, 2021, pp. 1–6, doi: 10.1109/FUZZ45933.2021.9494538.

[22] G. G. Rigatos and S. G. Tzafestas, "Parallelization of a fuzzy control algorithm using quantum computation," *IEEE Trans. Fuzzy Syst.*, vol. 10, no. 4, pp. 451–460, Aug. 2002, doi: 10.1109/TFUZZ.2002.800690.

[23] L. Visintin, A. Maron, R. Reiser, and V. Kreinovich, "Aggregation operations from quantum computing," in *Proc. IEEE Int. Conf. Fuzzy Syst.*, 2013, pp. 1–8, doi: 10.1109/FUZZ-IEEE.2013.6622365.

[24] A. Ávila, M. Schmalfuss, R. Reiser, and V. Kreinovich, "Fuzzy Xor classes from quantum computing," in *Proc. Int. Conf. Artif. Intell. Soft Comput.*, 2015, pp. 305–317, doi: 10.1007/978-3-319-19369-4_28.

[25] A. Pourabdollah, G. Acampora, and R. Schiattarella, "Fuzzy logic on quantum annealers," *IEEE Trans. Fuzzy Syst.*, vol. 30, no. 8, pp. 3389–3394, Aug. 2022, doi: 10.1109/TFUZZ.2021.3113561.

[26] A. Pourabdollah, G. Acampora, and R. Schiattarella, "Implementing defuzzification operators on quantum annealers," in *Proc. IEEE Int. Conf. Fuzzy Syst.*, 2022, pp. 1–6, doi: 10.1109/FUZZ-IEEE55066.2022.9882576.

[27] G. Acampora, F. Luongo, and A. Vitiello, "Quantum implementation of fuzzy systems through Grover's algorithm," in *Proc. IEEE Int. Conf. Fuzzy Syst.*, 2018, pp. 1–8, doi: 10.1109/FUZZ-IEEE.2018.8491579.

[28] IBM Quantum, 2021. [Online]. Available: https://quantum-computing.ibm.com/

[29] M. A. Nielsen and I. Chuang, "Quantum computation and quantum information," USA: Cambridge University Press, 2011, doi: 10.1017/CBO9780511976667.

[30] P. W. Shor, "Polynomial-time algorithms for prime factorization and discrete logarithms on a quantum computer," *SIAM J. Comput.*, vol. 26, no. 5, pp. 1484–1509, Oct. 1997, doi: 10.1137/S0097539795293172.

[31] L. K. Grover, "A fast quantum mechanical algorithm for database search," in *Proc. 28th Annu. ACM Symp. Theory Comput.*, 1996, pp. 212–219, doi: 10.48550/arXiv.quant-ph/9605043.

[32] G. Acampora, F. Di Martino, A. Massa, R. Schiattarella, and A. Vitiello, "D-NISQ: A reference model for distributed noisy intermediate-scale quantum computers," *Inf. Fusion*, vol. 89, pp. 16–28, 2023, doi: 10.1016/j.inffus.2022.08.003.

[33] J. M. Mendel, "Fuzzy logic systems for engineering: A tutorial," *Proc. IEEE*, vol. 83, no. 3, pp. 345–377, Mar. 1995, doi: 10.1109/5.364485.

[34] G. Antonelli, S. Chiaverini, and G. Fusco, "A fuzzy-logic-based approach for mobile robot path tracking," *IEEE Trans. Fuzzy Syst.*, vol. 15, no. 2, pp. 211–221, Apr. 2007, doi: 10.1109/TFUZZ.2006.879998.

[35] P. Hajek, "Interpretable fuzzy rule-based systems for detecting financial statement fraud," in *Proc. IFIP Int. Conf. Artif. Intell. Appl. Innov.*, 2019, pp. 425–436, doi: 10.1007/978-3-030-19823-7_36.

[36] L. Magdalena, "Fuzzy rule-based systems," in *Springer Handbook of Computational Intelligence*, J. Kacprzyk and W. Pedrycz, Eds., Berlin, Germany: Springer, 2015, pp. 203–218, doi: 10.1007/978-3-662-43505-2_13.

[37] Z. Kovacic and S. Bogdan, *Fuzzy Controller Design: Theory and Applications*. Boca Raton, FL, USA: CRC Press, 2018.

[38] M. M. Gupta and J. Qi, "Theory of t-norms and fuzzy inference methods," *Fuzzy Sets Syst.*, vol. 40, no. 3, pp. 431–450, 1991, doi: 10.1016/0165-0114(91)90171-L.

[39] M. Schenk et al., "Hybrid actor-critic algorithm for quantum reinforcement learning at CERN beam lines," *Quantum Sci. Technol.*, vol. 9, no. 2, Feb. 2024, Art. no. 025012, doi: 10.1088/2058-9565/ad261b.

[40] G. Brockman et al., "OpenAI gym," 2016, *arXiv:1606.01540*, doi: 10.48550/arXiv.1606.01540.

[41] G. Acampora and R. Schiattarella, "Deep neural networks for quantum circuit mapping," *Neural Comput. Appl.*, vol. 33, no. 20, pp. 13723–13743, 2021, doi: 10.1007/s00521-021-06009-3.

[42] C. Bracco et al., "AWAKE: A proton-driven plasma wakefield acceleration experiment at CERN," *Nuc. Part. Phys. Proc.*, vol. 273–275, pp. 175–180, 2016, doi: 10.1016/j.nuclphysbps.2015.09.022.

[43] E. Adli et al., "Acceleration of electrons in the plasma wakefield of a proton bunch," *Nature*, vol. 561, no. 7723, pp. 363–367, 2018, doi: 10.1038/s41586-018-0485-4.

[44] E. Gschwendtner et al., "The AWAKE run 2 programme and beyond," *Symmetry*, vol. 14, no. 8, 2022, Art. no. 1680, doi: 10.3390/sym14081680.

[45] R. Agustsson et al., "Experimental studies of a high-gradient X-band welded hard-copper split accelerating structure," *J. Phys. D: Appl. Phys.*, vol. 55, no. 14, 2022, Art. no. 145001, doi: 10.1088/1361-6463/ac4632.

[46] Y. Chung, G. Decker, and K. Evans, "Closed orbit correction using singular value decomposition of the response matrix," in *Proc. Int. Conf. Part. Accel.*, 1993, pp. 2263–2265, doi: 10.1109/PAC.1993.309289.

[47] L.-X. Wang and J. M. Mendel, "Generating fuzzy rules by learning from examples," *IEEE Trans. Syst., Man, Cybern.*, vol. 22, no. 6, pp. 1414–1427, Nov./Dec. 1992, doi: 10.1109/21.199466.

[48] J.-S. Jang, "ANFIS: Adaptive-network-based fuzzy inference system," *IEEE Trans. Syst., Man, Cybern.*, vol. 23, no. 3, pp. 665–685, 1993, doi: 10.1109/21.256541.

Giovanni Acampora (Senior Member, IEEE) received the master's (honors) and Ph.D. degrees in computer science from the University of Salerno, Italy, in 2003 and 2007, respectively.

He is a Full Professor in Computer Science with the University of Naples Federico II, Naples, Italy. From 2013 to 2016, he was a Reader in Computational Intelligence with the School of Science and Technology, Nottingham Trent University, Nottingham, U.K. From 2012 to 2013, he was in a Hoofddocent Tenure Track in Process Intelligence with the School of Industrial Engineering and Information Systems, Eindhoven University of Technology, Eindhoven, The Netherlands. His main research interests include computational intelligence and quantum computing.

Dr. Acampora is the Chair of IEEE Standards Association (SA) 1855WG. He is an Editor-in-Chief for *Quantum Machine Intelligence* and an Associate Editor in various editorial boards. In 2017, he was the General Chair of IEEE International Conference on Fuzzy Systems. He has received the 2016 IEEE SA Emerging Technology Award, the 2019 Canada–Italy Innovation Award for Emerging Technologies, and the IBM Quantum Experience Academic Research Program Award. In 2024, his research group received a Fujitsu Quantum Challenge Award for a project on quantum fuzzy inference engines for interpretable and efficient control of smart cities. He received the Best Paper Award at 2012 U.K. Workshop on Computational Intelligence (Edinburgh, U.K.) and 2021 IEEE International Conference on Fuzzy Systems.

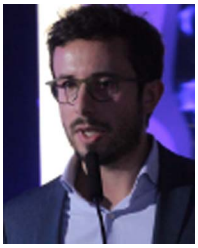

Michele Grossi received the industrial Ph.D. degree in high energy physics from the University of Pavia, Pavia, Italy, in 2021.

He is currently a Senior Fellow in Quantum Computing with the European Organization for Nuclear Research (CERN), Meyrin, Switzerland. He was a Quantum Technical Ambassador with IBM, Zurich, Switzerland, and a Hybrid Cloud Solution Architect. In his current role, he co-supervises QML projects with CERN IT Innovation. His research interests include the development of QML pipelines for high-energy physics (HEP) problems and their usage in different fields.

Michael Schenk received the Ph.D. degree in particle accelerator physics from the École Polytechnique Fédérale de Lausanne (EPFL), Lausanne, Switzerland, in 2019.

During his Ph.D. research, he developed a novel Landau damping technique for beam instability mitigation in circular particle colliders. Following his postdoctoral research with EPFL, where he worked on machine learning for beam lifetime prediction, he is currently a Senior Fellow with the European Organization for Nuclear Research, Meyrin, Switzerland. His main research activities lie in developing algorithms and automatic solutions for particle accelerator operation within the Beams Controls Software and Services group. His research interests include sample-efficient reinforcement learning and its application to real-world problems.

Roberto Schiattarella (Student Member, IEEE) received the Ph.D. degree in quantum technologies from the University of Naples Federico II, Naples, Italy, in 2023, with a thesis titled "Quantum computational intelligence."

His current research interests include quantum computational intelligence algorithms and their possible real-world applications, as well as classical computational intelligence algorithms to improve the current state of quantum computers.

Dr. Schiattarella received the IEEE Computational Intelligence Society Graduate Student Research Grant in 2022. He was in the research group that received a Fujitsu Quantum Challenge Award for a project on quantum fuzzy inference engines for interpretable and efficient control of smart cities.